UCRL-JRNL-205457

Long period Variables In the LMC: Results from ACHO and 2MASS

O.J. Fraser, S.L. Hawley, K.H. Cook, S.C. Keller

07-30-04

This work was performed under the auspices of the U.S. Department of Energy by University of California, Lawrence Livermore National Laboratory under Contract W-7405-Eng-48.

Long Period Variables In the LMC: Results from MACHO and 2MASS

Oliver J. Fraser, Suzanne L. Hawley

Department of Astronomy, University of Washington Box 351580, Seattle WA, 981951580

fraser@astro.washington.edu, slh@astro.washington.edu

Kem H. Cook

IGPP, Lawrence Livermore National Laboratory MS L413 P.O. Box 808 Livermore, CA 94550

kcook@llnl.gov

Stefan C. Keller

Research School of Astronomy and Astrophysics Australian National University Mount Stromlo Obs. Cotter Rd., Weston, ACT 2611, Australia

stefan@mso.anu.edu.au

ABSTRACT

We use the eight year lightcurve database from the MACHO (MAssive Compact Halo Objects) project together with infrared colors and magnitudes from 2MASS (the Two Micron All Sky Survey) to identify a sample of 22,000 long period variables in the Large Magellanic Cloud (referred to hereafter as LMC LPVs). A periodluminosity diagram of these stars reveals six welldefined sequences, in substantial agreement with previous analyses of samples from OGLE (Optical Gravitational Lensing Experiment). In our analysis we identify analogues to galactic LPVs in the LMC LPV sample. We find that carbondominated AGB stars populate only two of the sequences, one of which includes the Mira variables. The highluminosity end of the same two sequences are also the location of the only stars with $J - K_S > 2$, indicating that they are enshrouded in dust. The unknown mechanism that produces the variability of the last sequence – those stars with long secondary periods – produces di_erent morphology in the periodluminosity diagram than what is seen in the first four sequences, which are thought to be caused by pulsation. In particular, the last sequence extends to lower luminosity RGB stars and the luminosity

function does not peak among the AGB stars. We point out several features which will constrain new models of the periodluminosity sequences.
Subject headings: galaxies: individual (LMC) — stars: AGB and postAGB — stars: variables: other

1. Introduction

Long period variables (LPVs) are giant stars that pulsate with periods ranging from weeks to years. The prototypical case is Mira (Omicron) Ceti, from which all largeamplitude (> 2.5 magnitudes in V) regular LPVs take their name. LPVs are typically asymptotic giant branch (AGB) stars that are in the late stages of stellar evolution, where the pulsation mechanism(s) – and the relationships between pulsation, mass loss, and the eventual ejection of the stellar envelope as the star becomes a planetary nebula – are all poorly understood. During this relatively short AGB phase, stars manage to lose a significant fraction of their total mass, returning processed material to the interstellar medium. A qualitative picture of the massloss process invokes instabilities in the helium and hydrogen burning shells surrounding the degenerate core of the star. This provides the energy for a variety of stellar pulsation modes, causing shocks in the envelope which lift material high in the atmosphere. The temperature is then low enough to allow the formation of dust, which is subsequently ejected from the atmosphere by radiation pressure from the luminous core. Pulsations – which a_ect both the radius and temperature of the star – together with the shocks and dust formation, combine to produce significant photometric variability.

The study of LPVs has undergone a recent revival with the advent of surveys producing large catalogs of variable stars. Gravitational microlensing surveys, such as OGLE – Paczynski et al. (1994) and OGLE II – Udalski, Kubiak, & Szymanski (1997); EROS – Aubourg et al. (1995); MACHO – Alcock et al. (1997); and MOA – Bond et al. (2001) require that millions of stars be imaged nightly. The variable star catalogs that arise as a byproduct contain thousands of stars with light curves covering several thousand days.

As noted by Cook et al. (1996) the long period variables in the MACHO database form five parallel sequences in periodluminosity space. Wood et al. (1999) classified these and suggested possible underlying mechanisms for the five. Our use of infrared magnitudes in the periodluminosity relations shown in Figure 1 reveals six sequences. Wood's second sequence ("B" in his notation) is split into our Sequences 2 and 3. In terms of our observed sequences, Wood et al. (1999) found that Sequence 4 corresponds to Mira type variables, which are theorized to be pulsating in the fundamental mode. Higherorder pulsations are invoked to explain the shorter period sequences (1,2, and 3). The sequence that was longerperiod and dimmer than the Miras (our Sequence 5) showed light curves that suggested that all

of these variable stars were eclipsing binaries. Stars in the longest period sequence (Sequence 6) proved more mysterious since the long secondary periods of these stars could not be explained by radial pulsations – they are longer than the periods of Miras, which themselves are theorized to be pulsating in the fundamental mode. Additionally, they all exhibited multiple periods with the short period associated with Wood's Sequence "B". This prompted Wood et al. to propose that Sequence 6 was caused by the eclipse of the AGB star by a cloud of material around an unseen companion.

More recent studies using OGLEII data [Ita et al. (2002); Kiss & Bedding (2003); Ita et al. (2004); Kiss & Bedding (2004)] have extended the work on the periodluminosity sequences. These authors showed that the use of infrared magnitudes for luminosity reveals two sequences from the original second sequence. Further, their data show that Wood's first two sequences (our first three sequences) exhibit a split in luminosity due to the contribution of red giant branch (RGB) stars.

In this paper we use the full eightyear MACHO database to reexamine the LPV periodluminosity relations. MACHO observations have several advantages over previous studies: the colors of MACHO light curves yield superior sampling of photometric variability of RGB stars, and the time baseline of the light curves is twice as long (eight years compared to four years).

2. Data

2.1. The MACHO LMC Variable Star Database

The MACHO project (Alcock et al. 1997) comprises eight years of observations of the Large and Small Magellanic Clouds and the Milky Way Bulge. Data were taken simultaneously in a red and a blue filter. In this work we only use data from the Large Magellanic Cloud. Variable star candidates were chosen from the full database of several million stars if the central 80 percent of points in the light curve failed to fit a constant magnitude in a _squared test. This criterion resulted in the 207,632 variable candidates that appear in the MACHO variable star catalog (Alcock et al. 2003).

MACHO employed a nonparametric phasing technique (Riemann 1994) to find periods for each candidate variable star. Data from the red and the blue light curves were analyzed independently, and a period and amplitude for each variable candidate were found in each dataset. There is no substantial di_erence between the periods found, but a plot of the red versus the blue amplitudes shows a bias toward larger amplitudes in the blue. We adopt the blue periods and amplitudes so that the wider spread in amplitude will allow us to better

discriminate types of LMC LPVs. The periodfinding algorithm tends to alias noisy data and stars with chaotic variability. Thus, stars with period aliases at the total survey length, one year, and multiples of one day, in particular up to the fourth multiple and down to oneninth (1 9) of a day, were all removed from the catalog. Note that these alias cuts result in blank vertical stripes in the periodluminosity diagram (Figure 1). Only 52 percent of the LPVs have well-determined periods, a total of 21,441 stars. We are currently analyzing the 20, 000 LPVs with poorlydetermined periods with the goal of understanding the multiperiodic nature of these stars.

The amplitudes in the MACHO database are determined from the di_erence between the median of five points nearest the maximum and five points nearest the minimum in the light curve. A model light curve is used to identify the times of maximum and minimum light, so stars that are not well fit by the model will tend to average to zero amplitude. Thus, noisy or chaotic data will not be assigned meaningful amplitudes.

2.2. 2MASS Photometry

The Two Micron All Sky Survey (2MASS) measured *J*, *H*, and K_s magnitudes for approximately half a billion objects over the entire sky (Cutri et al. 2003). The sky coverage, resolution, and sensitivity of 2MASS make it a very useful source of infrared magnitudes. We have matched the MACHO and 2MASS data by position for LMC LPVs with welldetermined periods. Since the 2MASS magnitudes were taken at random phases we expect scatter in the *K*magnitudes from the intrinsic variability of these LPVs. Although most of the stars in our sample are small amplitude pulsators and contribute a negligible amount of scatter in the K_s band, some of the stars that make up Sequence 4 are Mira variables. Miras are the largest amplitude LPVs and have a typical *K*amplitude of 0.6 (Wood 2000). Thus the 2MASS magnitudes of the largest amplitude stars may deviate from the mean by as much as 0.3 mags. We accept this as a source of scatter, and, assuming all LMC stars are at the same distance, we use the 2MASS K_s magnitude as our primary luminosity indicator.

Infrared magnitudes can also be used to distinguish the state of late AGB stars. After evolving through the RGB and horizontal branch, stars begin to ascend the AGB with a high O/C ratio in their atmospheres. These oxygenrich AGB stars include both the socalled early AGB stars and AGB stars that have had their first thermal pulses. Low mass stars will remain on the AGB long enough that thermal pulses initiate the "third dredgeup", the deepening of their convection zones down into material enriched in ^{12}C. The spectral type then changes to a carbon star. The objectiveprism survey of the LMC by Kontizas et al. (2001) showed that carbon stars appear on the infrared colorcolor diagram in a red tail running from the stellar locus. Infrared color cuts of $J - H > 0.89$ and $H - K_s > 0.32$ isolated 83% of the carbon stars in their sample, with only a nine percent contamination rate. A single color cut in $J - K_s$ can also select these stars since it is perpendicular to the tail of carbon stars; the result is a sample that is less complete but also has less contamination. In addition, the 2MASS colormagnitude diagram of the LMC (Nikolaev & Weinberg 2000) shows a clear division at $J - K_s = 1.4$ due to carbon stars. In this paper we will draw particular attention to LPVs near this color boundary, with the caveat that we are missing some twenty percent of the carbon stars, those that are warm and hence bluer than $J - K_s = 1.4$.

Nikolaev & Weinberg (2000) also find a population of very red stars, those with $J - K_s > 2$, that lie along the reddening vector from the carbon stars and are located in dusty regions of the LMC. They propose that these stars are surrounded by a dusty circumstellar envelope. Both AGB stars and at least a few protostars are known to lie in this region. Although such dusty LPV are likely to be very late AGB stars, pinpointing the exact evolutionary state of these latter stars will require a better understanding of the connection between massloss, pulsation, and the late stages of AGB star evolution.

3. Discussion

Periodluminosity relations for variable stars in the LMC are shown in Figure 1. The two Cepheid sequences are clearly visible between $0 < \log P < 1$ and $13 < K_s < 16$. When plotted in K_s, as shown here, it is evident that Wood's original sequences split in both period and luminosity. It also appears that the low luminosity ends of the first three sequences are o_set to longer periods. These e_ects have been previously seen in OGLE II data; Kiss & Bedding (2003), Ita et al. (2004). In this work we will refer to each sequence by number as denoted in Figure 1. The lower luminosity stars in Sequences 1, 2, and 3 have been identified as RGB stars (Kiss & Bedding 2004) using an analysis of the second derivative of the luminosity function. The number of stars located above and below the tip of the RGB ($K_s = 12.3 \pm 0.1$ for the LMC, Nikolaev & Weinberg (2000)) in each pulsation sequence are given in Table 1.

3.1. Connections Between LMC and Galactic LPVs

Galactic LPVs are identified primarily in The General Catalog of Variable Stars (Kholopov et al. 1996) which has traditionally classified LPVs by their *V* band behavior. The classification scheme, tabulated in Table 2, seperates LPVs into Mira types and classes of semiregular (SR) variables. Mira variables are defined as those pulsating with a period greater than 80 days and an amplitude of at least 2.5 in *V*. Whereas Mira variables show regular and strong periodicity, one would imagine that "semiregular" variables would have weak or poorly defined periods. Indeed, SRb stars have poorly expressed periodicity, *or* multiple periods, *or* only occasional periodicity, *or* chaotic pulsation. However, SRa stars are not necessarily semiregular at all; they are similar to Miras but with smaller amplitudes (Lebzelter, Schultheis, & Melchior 2002).

Due to the empirical nature of the GCVS classification system, connections drawn to the observed LMC LPV periodluminosity sequences are often not simple or direct. However, connections can be made; Lebzelter et al. (2002) find that Miras in the Galaxy and in the Magellanic Clouds have the same periodluminosity relationship, implying that the pulsation mechanism is not strongly dependent on metallicity.

Figure 2 shows LMC LPVs of di_erent amplitudes located in periodluminosity space, Table 1 gives the mean and maximum pulsation amplitudes for each sequence. There is only a small di_erence between our B_{MACHO} amplitudes and the *V* band amplitudes used to classify Galactic variables. Bessell & Germany (1999) found transformations from MACHO magnitudes to Cousins *V* and *R*. For $B_{MACHO} - R_{MACHO} > 1.0$

$$V - B_{MACHO} = -0.07 - 0.10(B_{MACHO} - R_{MACHO}). \quad (1)$$

The change in the amplitude then, is due to color changes during the star's variability cycle. In particular the change in the amplitude between *V* and B_{MACHO} is restricted to 10% of the color change in the MACHO photometric system.[1]

With reference to the LMC LPVs in Figure 2, Sequence 4 is composed on the long period side by Miras. Cioni et al. (2001) found that higher amplitude SRa stars lie on Sequence 4 with the Miras; low amplitude SRas, on the other hand, lie on the shorter period sequences (Sequences 1, 2, and 3). Cioni et al. (2001) investigate stars from Sequence 6 and find that they are all multiplyperiodic SRb stars. Wood et

al. (1999) found that the shorter period of these stars usually fell on his sequence “B”, which corresponds to our Sequences 2 and 3. Although this work did not identify any stars from Sequence 6 with a primary period on Sequence 1 this may be caused selection e_ect due to the small amplitude of pulsation on this sequence. Unlike sequence 4, the highest amplitude stars fall on the shorter period side of the sequence.

The RGB stars at the low luminosity end of Sequences 1 and 2 are low amplitude pulsators, and a similar set of stars is visible at the base of the Sequence 6. The latter sequence’s stars are particularly interesting as their pulsation mechanism remains unknown. Sequence 6 is also notable for a significant number of high amplitude variables (1 $< B_{amp} <$2.5).

3.2. Color and Luminosity Functions

Figure 3 shows LMC LPVs of di_erent $J - K_s$ color located on the periodluminosity diagram; as discussed in 2.2, stars with $J - K_s > 1.4$ are likely to be carbon stars, while stars with

§

$J - K_s >$2 are likely obscured by dust. Interestingly, the most heavily obscured stars lie only at the high luminosity end of Sequence 4 and are Mira types. The majority of carbon stars lie at the high luminosity end of Sequences 3 and 4. Sequence 6 shows that the lower luminosity, small amplitude pulsators visible in Figure 2 also have bluer colors than the rest of the sequence, again indicating a separate RGB population.

The colormagnitude diagrams and luminosity functions for each sequence are shown in Figure 4; the luminosity functions are scaled relative to the total population of stars in each sequence. The background distribution in the colormagnitude diagram is for the entire MACHO variable star catalog, whereas the background *luminosity function* is for *all* LMC stars measured by 2MASS (Nikolaev & Weinberg 2000).

The “bumps” in the luminosity function for each sequence correspond to particular populations at di_erent stages of stellar evolution. The tip of the RGB is the largest such bump, and was found by Nikolaev & Weinberg (2000) to be $K_s = 12.3 \pm 0.1$. Sequences 1 and 2 show

a substantial contribution from the tip of the RGB, whereas Sequences 3 and 4 are composed primarily of stars on the AGB (which overlaps with the RGB at this magnitude). Sequences 1, 2, 3, and 4 all show a peak in the luminosity function at K_S 11.3; this peak in variable AGB stars is not seen in the

Since we know the typical color of AGB stars, B_{MACHO} R_{MACHO} 1.5 (Alcock et al. 1999), we note that V magnitudes will be 0.22 brighter than the B_{MACHO} magnitudes.

overall LMC luminosity function (Nikolaev & Weinberg 2000).

The types of stars in each sequence are obtained by comparison with the colormagnitude diagram of the LMC from Nikolaev & Weinberg (2000). Sequences 1 and 2 have similar distributions including a population at the tip of the RGB as well as oxygenrich AGB stars. The stars with K_S < 10.5 are young, massive, AGB stars; they are most commonly found in Sequence 2. Sequences 3 and 4 also have similar populations, with both oxygenrich AGB stars and a large contribution from carbon stars. Sequence 4 extends further to the red in J K_S, probably due to dust obscuration around those stars. There are very few young, massive AGB stars in these sequences. Sequence 5 is dominated by RGB stars, as can be seen from both its luminosity function and position in the colormagnitude diagram. This is expected if it is composed of eclipsing binaries. Both Sequence 5 and 6 lack high luminosity young, massive AGB stars and the AGB dominated population that produces the significant peak in the luminosity function at K_S 11.3 in Sequences 1, 2, 3, and 4. Interestingly, Sequence 6 ends abruptly at K_S 13.7 (Sequence 5 is artificially cut o_ at K_S = 14.5). There is no feature in the “deep” LMC colormagnitude diagram (Nikolaev & Weinberg 2000) associated with this position, or with the bottom of the first four sequences. The di_erence in the low-luminosity cuto_ of Sequence 6 compared with the first four sequences, as well as the lack of a bump in the luminosity function at K_S 11.3 in Sequence 6, suggests that the variability is caused by a di_erent mechanism than the radial pulsation modes proposed to explain Sequences 1, 2, 3, and 4.

3.3. Comparisons to Theory

Explanations of the structure in the periodluminosity diagram often invoke radial pulsations, with parallel sequences indicating populations of overtone pulsators. We have plotted the linear, radial, nonadiabatic pulsation models of Wood & Sebo (1996) with our LMC

LPV data in Figure 5. These models were forced to fit the observed Mira periodluminosity relation of Feast et al. (1989). Note that the observed Mira relation lies precisely where we see the largest amplitude pulsators in Figure 2. Sequences 1, 2, 3, and 4 have all been previously attributed to overtone pulsations, but it is clear that Sequence 1 lies at periods that are too short to be described by these models. As discussed in Ita et al. (2004), the gap between Sequences 1 and 2 is also di_cult to explain in the context of overtone pulsations. Sequences 1 and 2 share every important feature discussed in this paper – morphology in the colormagnitude diagram; their luminosity function; infrared colors; and, to a lesser degree, amplitudes (see Table 1). The only substantial di_erence between Sequences 1 and 2 seems to be their periods, but an explanation using only higher overtone pulsations would have to explain why modes that lie in the gap between the two are preferentially damped.

Sequence 6 was originally theorized by Wood et al. (1999) to be caused by eclipses from a dustenshrouded unseen companion. This hypothesis required that $\sim$ 25% of AGB stars exist in semidetached binaries. Wood, Olivier, & Kawaler (2004) have recently completed an analysis of four years of echelle data for three Galactic stars with long secondary periods (examples of which are tabulated in Houk (1963)). Additional photometric data for 111 stars from MACHO allow them to investigate, and rule out, explanations involving solely radial pulsations, nonradial pulsations, orbiting companions, nonspherically symmetric stars, dust obscuration, and chromospheric activity. They propose that the most likely explanation is a lowdegree g^+ mode in an extraordinarily thick radiative layer, which would allow large amplitudes at the stellar surface, combined with largescale star spot activity.

4. Conclusions and Future Work

The combination of observations over a long time baseline, accurate optical photometry extending below the tip of the RGB, and 2MASS infrared photometry has allowed us to place multiple constraints on the stars inhabiting each of the sequences observed in the periodluminosity diagram of the LMC.

- Most of the LPVs in this analysis, which comprises the 52% of LMC LPVs with welldetermined periods, are SRa stars or Miras. The amplitude criterion ($\Delta V > 2.5$ for Miras) used to di_erentiate Galactic SRa and Mira stars seems arbitrary, as SRa's and Miras overlap in our diagrams. Stars from Sequence 6 never have an isolated period, thus marking them as SRb stars.
- Our periodluminosity Sequences 1 and 2 both show low luminosity extensions comprised of RGB stars, and have AGB

stars that are oxygen rich ($J - K_S < 1.4$). As discussed in § 2.2 this implies that these AGB stars haven't yet undergone the third dredgeup. Compared with the significant population of redder (carbon) stars in Sequences 3 and 4 this implies that older stars are segregated to the latter two sequences. The populations of young, massive AGB stars in Sequences 1 and 2 that are identified in Figure 4 (See 3.2) support this hypothesis.

- The shortest period sequence (Sequence 1) stands out because it is offset further from the next closest sequence than the others. The short periods of Sequence 1 make it difficult to fit with standard radial pulsation models.
- Sequences 5 and 6 tend to follow the LMC luminosity function more closely than the others, indicating that they are more nearly drawn from the population of giant stars in the LMC. In particular, neither sequence shows a "bump" in its luminosity function due to AGB stars, unlike Sequences 1, 2, 3, and 4. These characteristics suggest that a different mechanism produces the variability of these sequences. Sequence 5 is likely populated by eclipsing binary systems.
- Although the physical mechanism that causes Sequence 6 is still elusive, there are numerous constraints on possible models. These include the ubiquity of multiple periods and the luminosity function behavior already discussed. In addition the AGB population in this sequence

  exhibits higher amplitude pulsation on its shorter period side, opposite what is found for Sequence 4. Sequence 6 has a significant low luminosity component that, compared with the RGB star component of Sequences 1, 2, and 3, is bluer, extends to lower luminosity, and is broader in period.

We are currently analyzing the 20,000 multiply periodic LMC LPVs that are not included in the present sample, with the goal of understanding the relationships between the periodluminosity sequences and the positions in periodluminosity space of stars at various stages of their evolution. This will both increase our sample size and allow us to better analyze how these sequences are related.

This paper utilizes public domain data obtained by the MACHO Project, jointly funded by the US Department of Energy through the University of California, Lawrence Livermore National Laboratory under contract No. W7405Eng48, by the National Science Foundation through the Center for Particle Astrophysics of the University of California under cooperative agreement AST8809616, and by the Mount Stromlo and Siding Spring Observatory, part of the Australian National University.

This work was performed under the auspices of the U.S. Department of Energy, National Nuclear Security Administration by the University of California, Lawrence Livermore National Laboratory under contract No. W7405Eng48.

This publication makes use of data products from the Two Micron All Sky Survey, which is a joint project of the University of Massachusetts and the Infrared Processing and Analysis Center/California Institute of Technology, funded by the National Aeronautics and Space Administration and the National Science Foundation.

Oliver Fraser and Suzanne Hawley acknowledge support by NSF grant AST 0205875.

REFERENCES

Alcock, C., et al. 1997, ApJ, 486, 697 —. 1999, PASP, 111, 1539 —. 2003, VizieR Online Data Catalog, 2247, 0 Aubourg, E., et al. 1995, A&A, 301, 1 Bessell, M. S., & Germany, L. M. 1999, PASP, 111, 1421 Bond, I. A., et al. 2001, MNRAS, 327, 868 Cioni, M.R. L., et al. 2001, A&A, 377, 945 Cook, K., et al. 1996, in Proceedings of the 12th IAP Astrophysics Meeting, Variable Stars and The Astrophysical Returns of Microlensing Surveys, ed. R. Ferlet, J. Maillard, & B. Raban (GifsurYvette, France: Editions Fronti´eres), 17

Cutri, R. M., et al. 2003, VizieR Online Data Catalog, 2246, 0

Feast, M. W., Glass, I. S., Whitelock, P. A., & Catchpole, R. M. 1989, MNRAS, 241, 375

Houk, N. 1963, AJ, 68, 253

Ita, Y., et al. 2002, MNRAS, 337, L31

—. 2004, MNRAS, 347, 720

Kholopov, P. N., et al. 1996, VizieR Online Data Catalog, 2139, 0

Kiss, L. L., & Bedding, T. R. 2003, MNRAS, 343, L79

—. 2004, MNRAS, 347, L83

Kontizas, E., Dapergolas, A., Morgan, D. H., & Kontizas, M. 2001, A&A, 369, 932

Lebzelter, T., Schultheis, M., & Melchior, A. L. 2002, A&A, 393, 573

Nikolaev, S., & Weinberg, M. D. 2000, ApJ, 542, 804

Paczynski, B., Stanek, K. Z., Udalski, A., Szymanski, M., Kaluzny, J., Kubiak, M., Mateo, M., & Krzeminski, W. 1994, ApJ, 435, L113

Riemann, J. 1994, PhD thesis, University of California, Berkeley

Udalski, A., Kubiak, M., & Szymanski, M. 1997, Acta Astronomica, 47, 319

Wood, P. R. 2000, Publications of the Astronomical Society of Australia, 17, 18

Wood, P. R., Olivier, E. A., & Kawaler, S. D. 2004, ApJ, 604, 800

Wood, P. R., & Sebo, K. M. 1996, MNRAS, 282, 958

Wood, P. R., et al. 1999, in IAU Symp. 191, Asymptotic Giant Branch Stars, ed. E. Le Bertre, A.

L´ebre, & C. Waelkens (San Francisco: Astronomical Society of the Pacific), 151

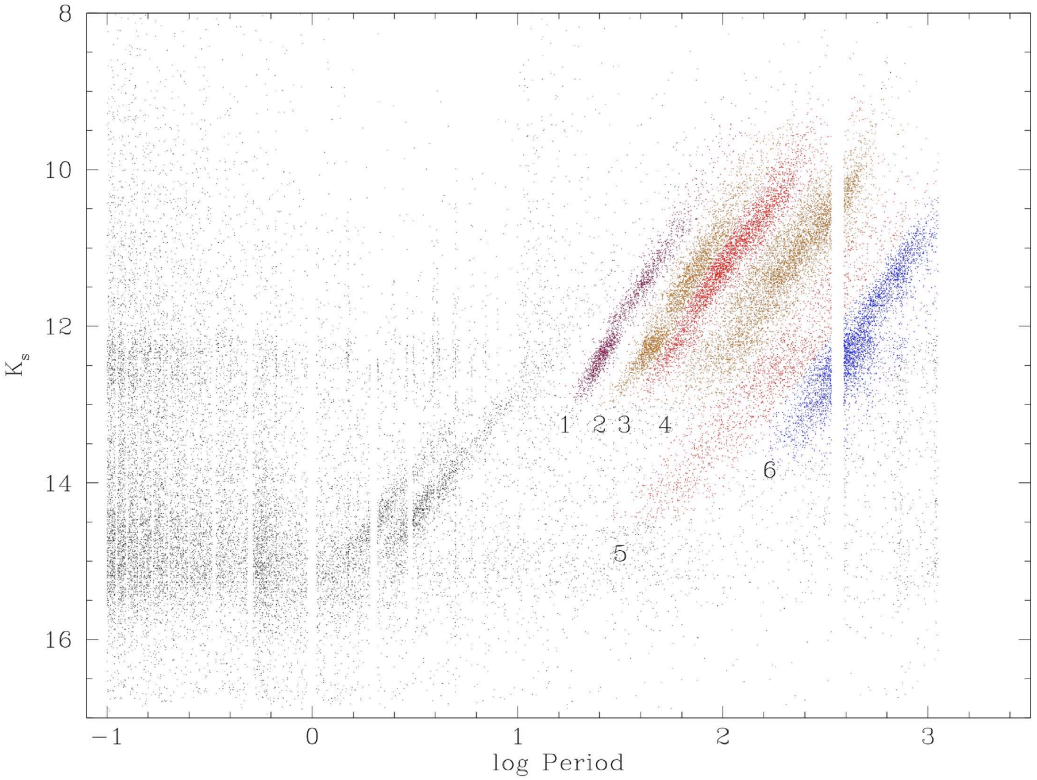

Fig. 1.— (top) LMC periodluminosity diagram showing the stars with welldetermined periods. The luminosity split at the top of the RGB (K_s = 12.3 $\pm$ 0.1) is observed in sequences 1, 2, and 3. Sequences 1, 2, 3, 5, and 6 show smooth distributions to much lower luminosity.

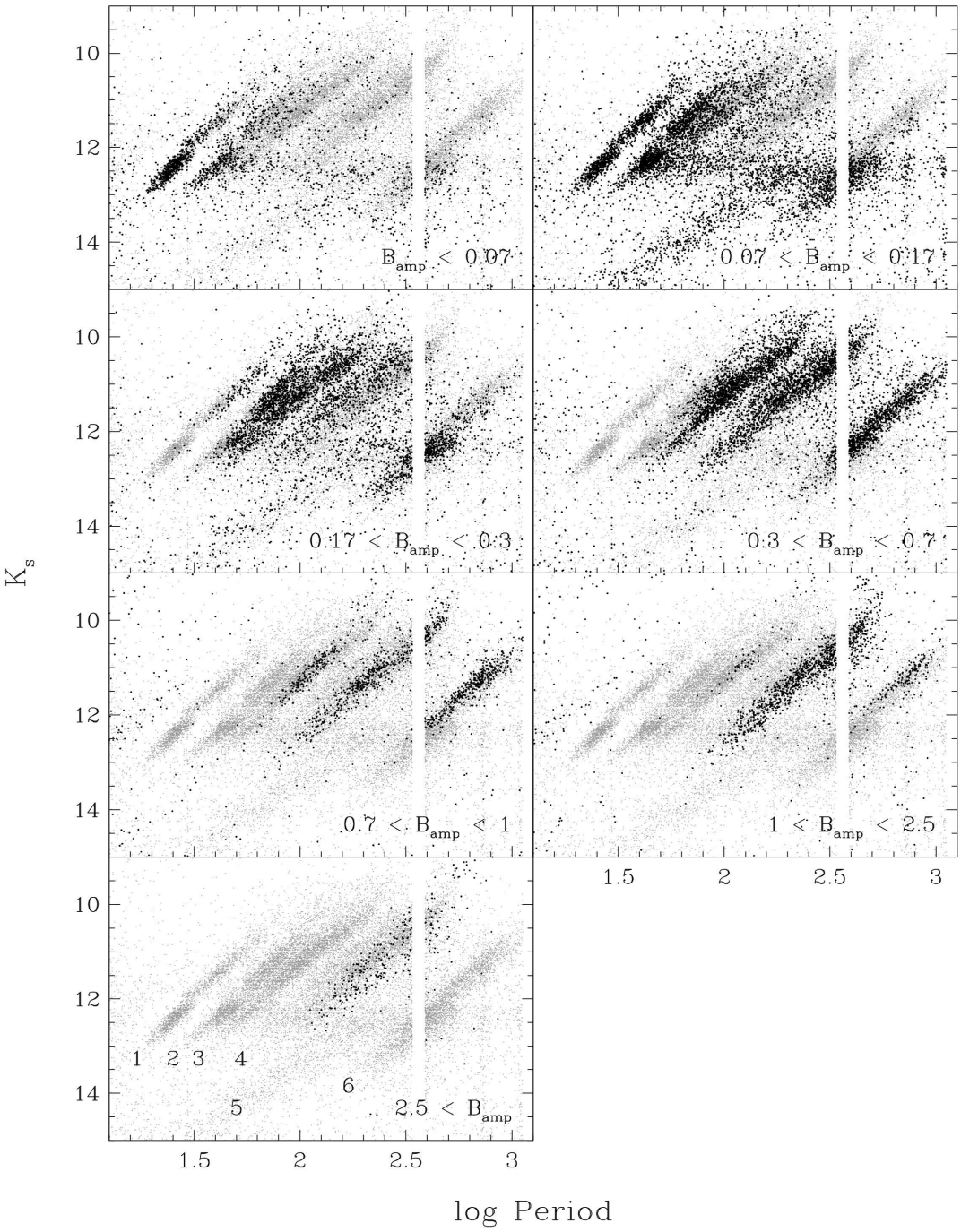
$B_{amp} < 0.07$
$0.07 < B_{amp} < 0.17$
$0.17 < B_{amp} < 0.3$
$0.3 < B_{amp} < 0.7$
$0.7 < B_{amp} < 1$
$1 < B_{amp} < 2.5$
$2.5 < B_{amp}$
1 2 3 4
5
6
10
12
14
1.5
2
2.5
3
K_s
log Period

Fig. 2.— PeriodLuminosity diagrams highlighting stars in seven amplitude bins (with divisions at B_{MACHO} = 0.07, 0.17, 0.3, 0.7, 1, and 2.5). The background distribution (in gray) is for all of the LMC LPVs from Figure 1 and is shown as a reference. Note that the highest amplitude stars are the Mira variables, located on the long period side of Sequence 4.

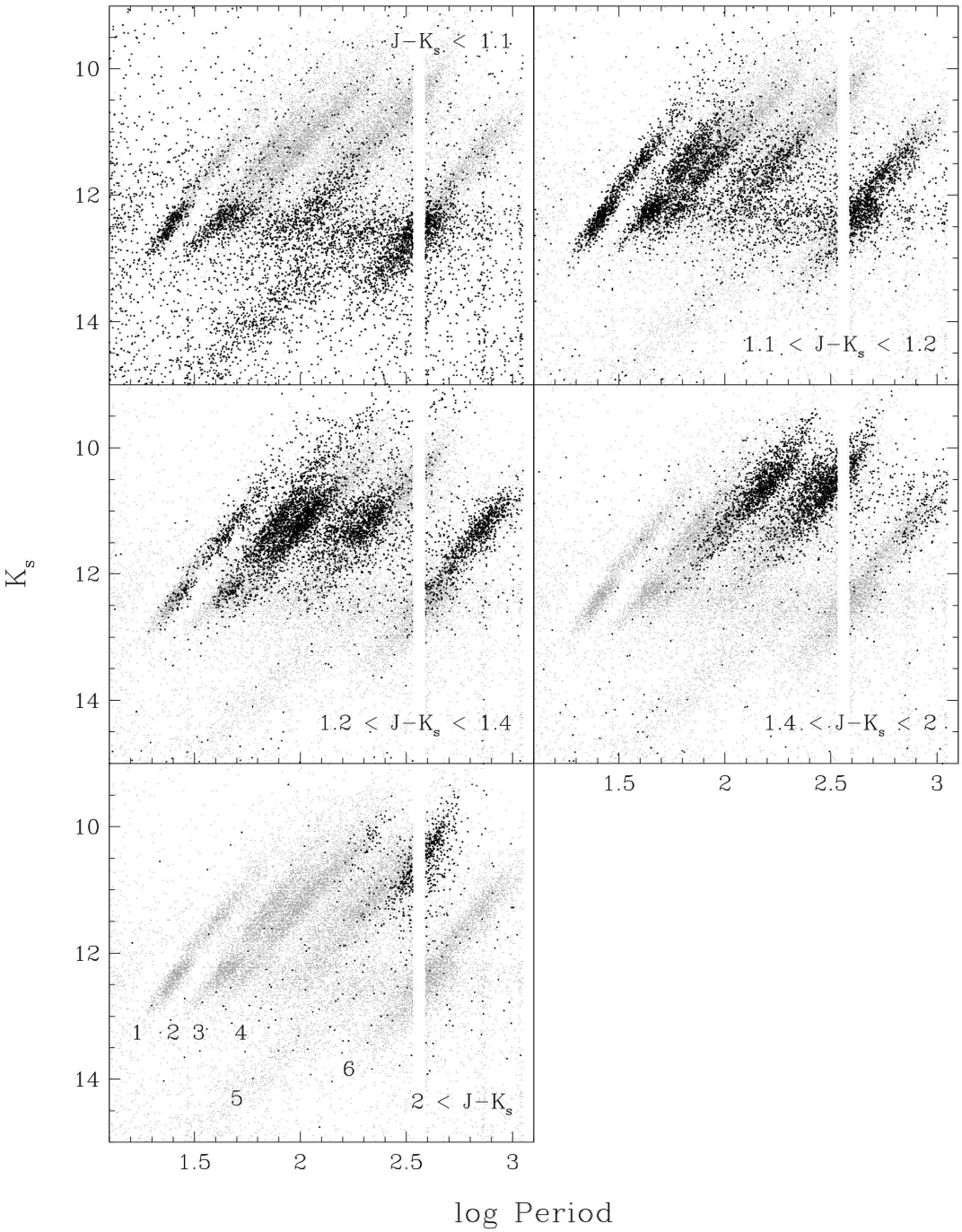
J−K$_s$ < 1.1
1.1 < J−K$_s$ < 1.2
1.2 < J−K$_s$ < 1.4
1.4 < J−K$_s$ < 2
2 < J−K$_s$
1
2
3
4
5
6
10
12
14
1.5
2
2.5
3
K$_s$
log Period

Fig. 3.— PeriodLuminosity diagrams highlighting stars in five $J - K_s$ color bins (with divisions at $J - K_s$ = 1.1, 1.2, 1.4, and 2). The background distribution (in gray) is for all of the LMC LPVs from Figure 1 and is shown as a reference. Note that stars with $J - K_s > 1.4$ are carbon stars, and stars with $J - K_s > 2$ are obscured by dust (See 2.2). The bluest stars ($J - K_s < 1.1$) show the

§

RGB populations of the periodluminosity sequences.

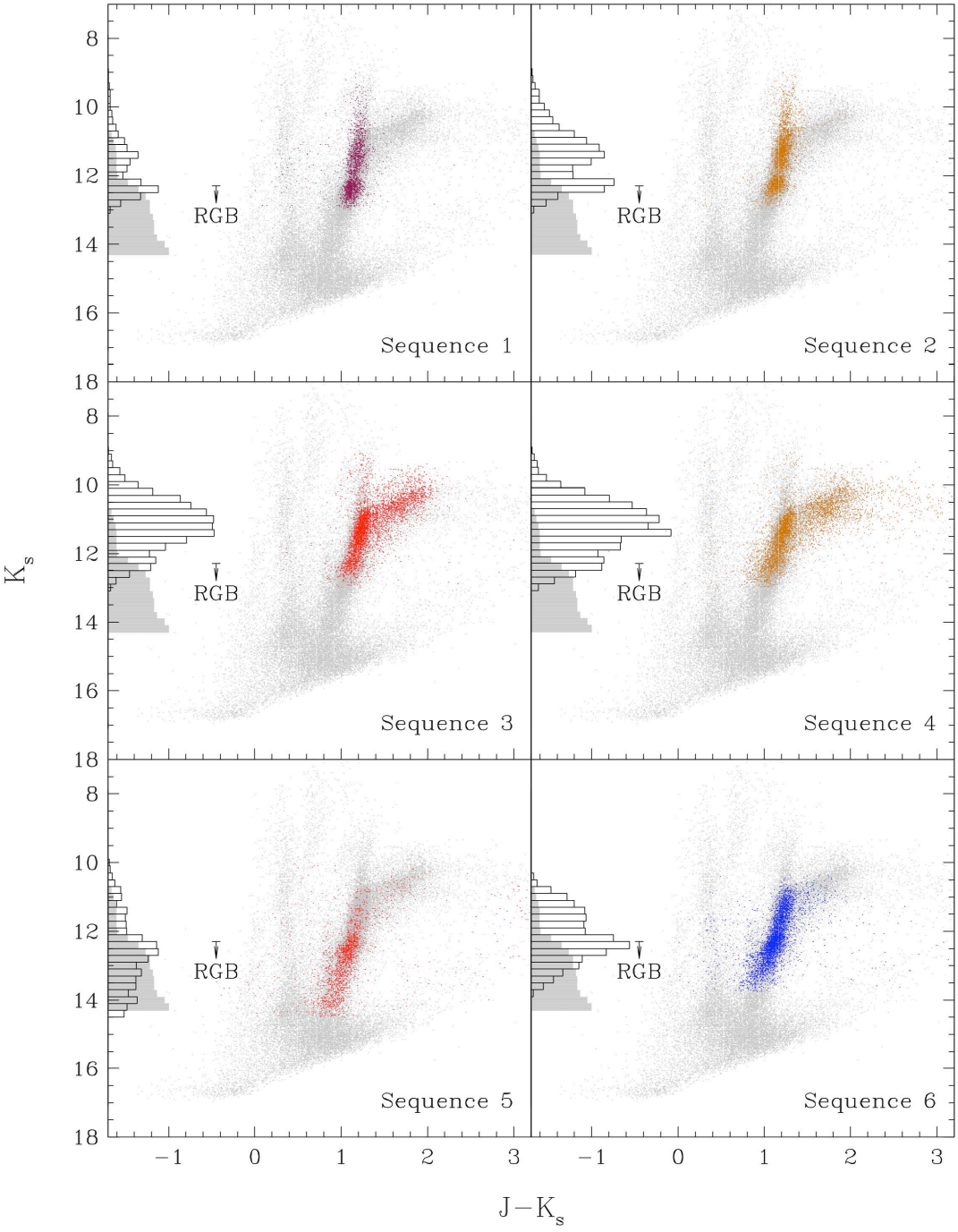
Sequence 1
Sequence 2
Sequence 3
Sequence 4
Sequence 5
Sequence 6
RGB
K_s
$J-K_s$
8
10
12
14
16
18
−1
0
1
2
3

Fig. 4.— Colormagnitude diagrams and luminosity functions (along the left vertical axes) for each sequence. The background distribution in the colormagnitude diagram is for the entire MACHO variable star catalog, whereas the background luminosity function is for *all* LMC stars measured by 2MASS.(Nikolaev & Weinberg 2000)

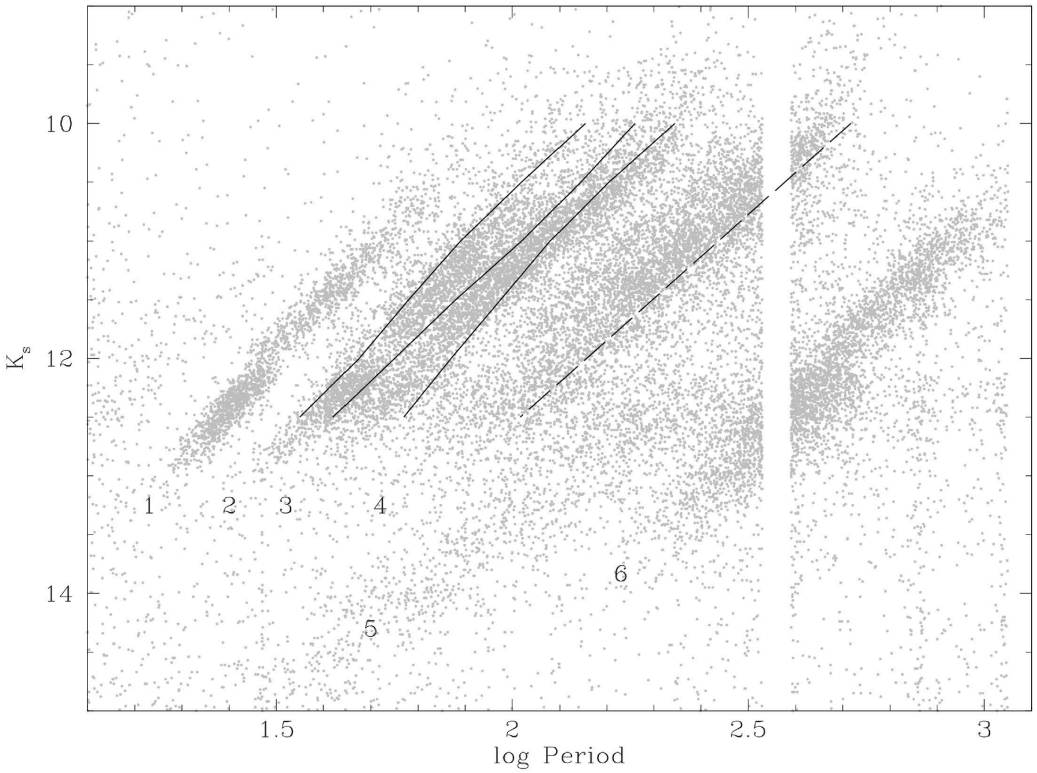
10
12
14
K_s
1
2
3
4
5
6
1.5
2
2.5
3
log Period

Fig. 5.— Periodluminosity diagram overlaid with the observed Mira relation of Feast et al. (1989) (dashed line) and the 3rd, 2nd, and 1st overtone (respectively, from left) models of Wood & Sebo (1996) (solid lines). The fundamental mode of the models was forced to fit the Mira relation of Feast et al. (1989).

Table 1. Properties of the PeriodLuminosity Sequences

Sequence	Star Count	Amplitude above TRGB[a]	below TRGB[a]	Mean[b]	Max
1	1337	673	0.11	1.75	
2	2780	540	0.17	1.90	
3	3967	310	0.34	3.79	
4	5009	628	0.77	8.04	
5	636	1384	0.28	4.47	
6	2163	1802	0.38	5.58	

[a] Tip of the Red Giant Branch; $K_S = 12.3 \pm 0.1$ in the LMC (Nikolaev & Weinberg 2000). Above the tip of the RGB the LPVs are all AGB stars.

[b] We are unable to estimate a minimum amplitude of pulsation as MACHO's amplitude finding algorithm reports *zero* amplitude for noisy or chaotic data (see § 2.1).

Table 2. GCVS Long Period Variable Classification

d (days)	Amplitude (V)	PL sequence(s)
35 – 1200	≥ 2.5	4
	< 2.5	1,2,3,4
	...	1,2,3,6
"al thousand"	_ 1	0.1 – 4
	...	...

[a] a "late" giant specifically indicates a spectral type of M, C, S, Me, Ce, or Se. [b] These rare types are not represented in our collection of late giants.